RSC Advances

ROYAL SOCIETY OF CHEMISTRY

www.rsc.org/advances

Graphical abstract

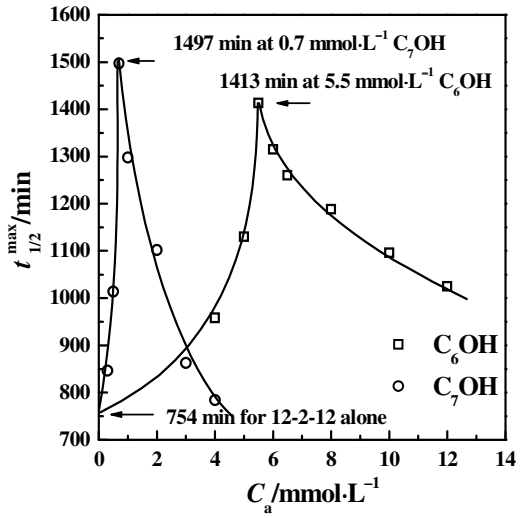

Highly stable foams were generated using a cationic gemini surfactant, ethanediyl-1, 2-bis(dodecyldimethylammonium bromide) (12-2-12) together with a linear alcohol, hexanol (C_6OH) or heptanol (C_7OH), in aqueous solution. There existing the optimum addition for both C_6OH and C_7OH.

Highly stable foams generated in mixed systems of ethanediyl-1, 2-bis(dodecyldimethylammonium bromide) and alcohols

Bing-Lei Song[1], Xiao-Na Yu[1], Jian-Xi Zhao[2*], Guo-Jing Sun[2]

1. The Key Laboratory of Food Colloids and Biotechnology, Ministry of Education, School of Chemical and Material Engineering, Jiangnan University, Wuxi, Jiangsu 214122, P. R. China

2. Institute of Colloid and Interface Chemistry, College of Chemistry and Chemical Engineering, Fuzhou University, Fuzhou, Fujian, 350108, P. R. China

Abstract: Stable foams were generated using a cationic gemini surfactant, ethanediyl-1, 2-bis(dodecyldimethylammonium bromide) (12-2-12) together with a linear alcohol, hexanol (C_6OH) or heptanol (C_7OH), in aqueous solution. The foam stability was determined using the half-life of foam height falling ($t_{1/2}$) as the index. The results showed that C_7OH was more efficient than C_6OH together with 12-2-12 to stabilize the foams. To generate the most stable foams, the optimum addition for both C_6OH and C_7OH was determined. The adsorption of the mixtures at the air/water interface was studied using surface tension measurements. The intermolecular interactions and the composition of the mixed monolayer were estimated by Rubingh-Rosen theory and the surface excess was derived from Gibbs equation. The total surface excess that included both 12-2-12 and alcohols, was shown to significantly increase following the addition of alcohols suggesting the active molecules were more densely packed at the interface. The interfacial dilational rheology of the films was examined using the oscillating drop technique. The results showed that a highly stable foam always corresponded to a highly elastic adsorption film. The present study suggests a new formula for the generation of highly stable foams using a gemini surfactant with a short spacer together with a linear alcohol.

Key words: Foam stability, interfacial adsorption, interfacial elasticity, alcohol effect

Corresponding author. Email: jxzhao.colloid@fzu.edu.cn

1. Introduction

Foams consist of gas bubbles separated by three-dimensional water channels and hence are metastable systems. Foam related technique such as microcellular foaming technology has been applied to produce polymeric foams with highly oriented and elongated cell structure[1]. It is known that the lifetime of an individual thin film that separates the two phases dominates the stability of foams. R. Krastev et al. reveal that the stability of foam films is related with the film thickness, the equilibrium of which is determined by the interplay of the dispersion attraction, electrical double-layer repulsion and short-range molecular interactions[2]. Surfactants are the most commonly added compounds used to stabilize foams by preventing bubbles in the foam from coalescing and allowing the lifetime of the film to be greatly increased. Pioneering studies strongly suggested that films which can effectively stabilize foams should possess excellent interfacial viscoelasticity and be of particularly high elasticity[3-13]. For example, D. Langevin et al. [13] investigated the stability of foams formed by several nonionic surfactants. The foam evolvement was found to be controlled by film elasticity at different stages. The high film elasticity usually corresponds to a dense structure of the adsorption monolayer, where the adsorbed surfactant molecules are tightly packed [8, 14, 15].

Gemini surfactant consists of two hydrophobic tails and two hydrophilic head-groups linked by a spacer per molecule[16]. It has been clear that the gemini structure of a short spacer can form a densely packed monolayer at the air/water interface[17]. In our previous studies, we have successfully constructed stable foams using gemini surfactants with a short spacer as stabilizers, such as ethanediyl-1, 2-bis(alkyldimethylammonium bromide) or 2-hydroxyl-propanediyl-1, 3-bis(alkyldimethylammonium bromide)[18-20]. Even so, however, there still remains gaps at the adsorption monolayers formed by the adsorbed gemini molecules due to the electrostatic repulsion. Consequently, the foam stability may be further enhanced if these gaps in the adsorption monolayers can be partly filled. To achieve this purpose, nonionic surfactants or linear alcohols with small head-groups may be effective additives. Many authors have studied the interactions of alcohols with ionic surfactants (including ionic gemini surfactants) and concluded that linear alcohols effectively promoted the ionic surfactant to form a dense adsorption monolayer[21-25]. However, to our knowledge, none of these studies focused on the relationship between foam stability and system composition. This work first reports highly stable foams generated in the

mixed systems of a gemini surfactant with a short spacer (12-2-12) and hexanol (C_6OH) or heptanol (C_7OH). The interfacial adsorption and the dilational viscoelasticity of the adsorbed films are characterized to explore the underlying mechanism. The presented system utilizes the advantages of gemini surfactant structure and provides a new formula of stable foam systems.

2. Experimental

2.1 Materials

Gemini surfactant, ethanediyl-1, 2-bis(dodecyldimethylammonium bromide) (abbreviated as 12-2-12), was synthesized in our laboratory and confirmed by ^{1}H NMR and elemental analysis (Supporting Information). Hexanol (C_6OH, AR) and heptanol (C_7OH, AR) were purchased from Sinopharm Chemical Reagent Co. Ltd (China). All solutions were prepared with Milli-Q water with a resistivity of 18.2 MΩ·cm.

2.2 Measurements

Foam stability was indexed by the half-life $t_{1/2}$. This was the time required for the collapse of the foam to half of its initial height according to Tehrani-Bagha and Holmberg' proposals[26] and was determined using the previously described setup[18]. Air with a constant flow speed of 68 mL·min^{-1} was bubbled through a porous glass disc fixed at the bottom of a cylindrical glass container (25 mm internal diameter, 140 mm height) filled with 5 mL of the test solution. Foam was produced until a height of 40 mm, *i.e.*, a volume of 20 cm^3, and the valve then shut immediately. The time needed for the collapse of the foam to half of its initial height was recorded. The experiments were repeated at least three times and all presented values were the means from these replicates. The temperature was kept at 25 ± 0.1 ^{o}C throughout the experiments using a water bath.

The surface tension of the surfactant aqueous solutions with or without additives was measured with a CHAN DCA-315 tension meter equipped with a Pt-Ir du Noüy ring to investigate adsorption at the air/water interface. The circumference of the ring was 5.930 cm. The ratio of the outside radius to the radius of the ring cross section (R/r) was 53.1218. The error of surface tension measurements was within 0.1 mN·m^{-1}.

Interface dilational rheology was measured using an optical angle meter OCA-20 with an

oscillating drop accessory ODG-20. The equilibrated interface was disturbed by sinusoidal oscillations. The accessible frequency range was 0.01−1Hz and the relative area (A) variation was ~6%. These conditions followed the range of linear viscoelasticity. Oscillations led to sinusoidal changes in the surface area and the radius, i.e. in the drop shape. The changes in drop shape were monitored by a CCD camera with a minimum of 50 frames per second. At the end of the experiment, the software retrieved the images and calculated the change in area and respective changes in surface tension for each cycle. Using Fourier transform analysis, the complex dilational modulus (ε*) and phase angle (θ) were determined and the dilational elasticity ε and dilational viscosity η were calculated by the relations

$$\varepsilon = |\varepsilon *| \cos\theta \quad (1)$$

$$\eta = \frac{|\varepsilon *|}{\omega} \sin\theta \quad (2)$$

3. Results and discussion

3.1 Foam stability

Fig.1 shows the semi-logarithmic plots of the characteristic decay time, $t_{1/2}$, against the surfactant (12-2-12) concentration, C_s, in the presence of hexanol (C_6OH) or heptanol (C_7OH). For all the systems, $t_{1/2}$ rapidly rose with increasing 12-2-12 concentration and plateaus over a narrow concentration range of c. 0.75−1.1 mmol·L^{-1} irrespective of the addition of C_6OH or C_7OH. These characteristic concentrations were close to their *cmc*s in the presence of the alcohols as discussed in Section 3.2. In contrast, the longest decay time of the foams, $t_{1/2,max}$, strongly depended on both the species and concentration of alcohols, which is more clearly shown in Fig.2. For each added alcohol, a sharp maximum appeared in the plot of $t_{1/2,max}$ versus C_a (the concentration of alcohol). Compared with that of 12-2-12 alone, the addition of alcohol could greatly enhance the foam stability and the $t_{1/2,max}$ attained 1413 min at 5.5 mmol·L^{-1} C_6OH and 1497 min at 0.7 mmol·L^{-1} C_7OH, which were two-fold higher than that (754 min) stabilized by 12-2-12 without additive[20]. Notably, the concentration of C_7OH to yield the maximum of $t_{1/2,max}$ was only one-fifth of C_6OH, indicating that C_7OH was a much more efficient additive to reform the foams stabilized by 12-2-12.

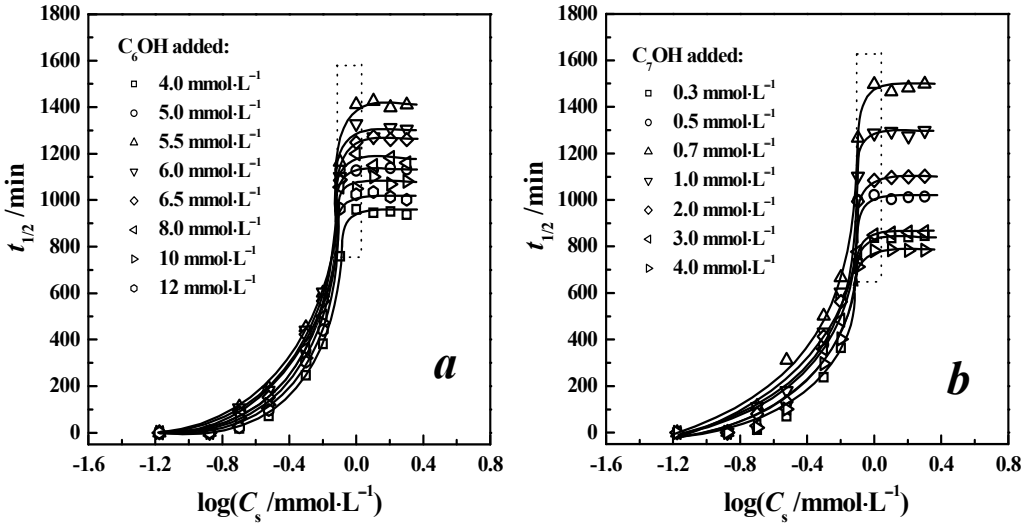

Fig.1 Semi-logarithmic plots of foam decay time, $t_{1/2}$, for foam height to fall by 50% as a function of 12-2-12 concentration in the presence of C_6OH (***a***) and C_7OH (***b***) at 25°C

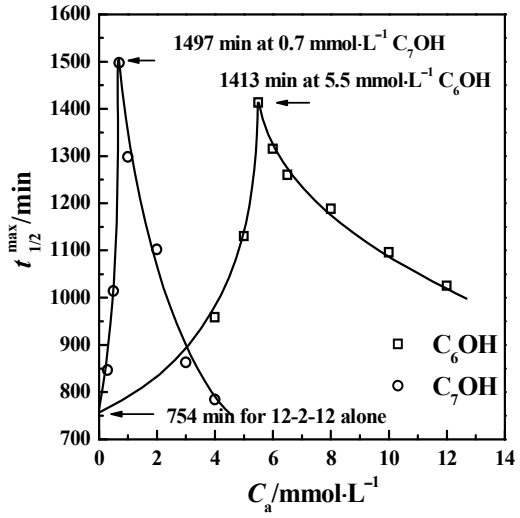

Fig.2 The maximum foam stability time $t_{1/2,max}$ as a function of the added quantity of alcohol: (squares) C_6OH and (circles) C_7OH

3.2 Surface tension curves

To understand the role of adding alcohols in stabilizing the foams, the surface tension of aqueous 12-2-12 solutions without and with different concentrations of alcohols was measured by the du Noüy ring technique. Fig.3 shows the semi-logarithmic plots of surface tension versus surfactant concentration. At low surfactant concentrations, the systems with alcohol exhibited smaller values of surface tension than that for 12-2-12-alone. This was attributed to the formation

of a mixed adsorption film that reduced the surface tension of water more effectively. From Fig.3, the critical micelle concentration (*cmc*) could be derived from the break point. The minimum surface tension (γ_{cmc}) at the *cmc* and the concentration (C_{20}) required to reduce a 20 $mN{\cdot}m^{-1}$ surface tension of water were also obtained. The three parameters characterized the ability of micelle formation and the effectiveness and the efficiency in surface tension reduction, respectively[27]. In the presence of alcohols, all three parameters were smaller than those generated by 12-2-12 alone (see Table 1), showing the synergistic effect of adding alcohols with 12-2-12. Comparatively, C_7OH was more synergistic than C_6OH with 12-2-12, which was also observed by Khan and colleagues[25]. Thus, the quantity of C_7OH required to produce identical synergism was considerably smaller than that of C_6OH as seen in Fig.3.

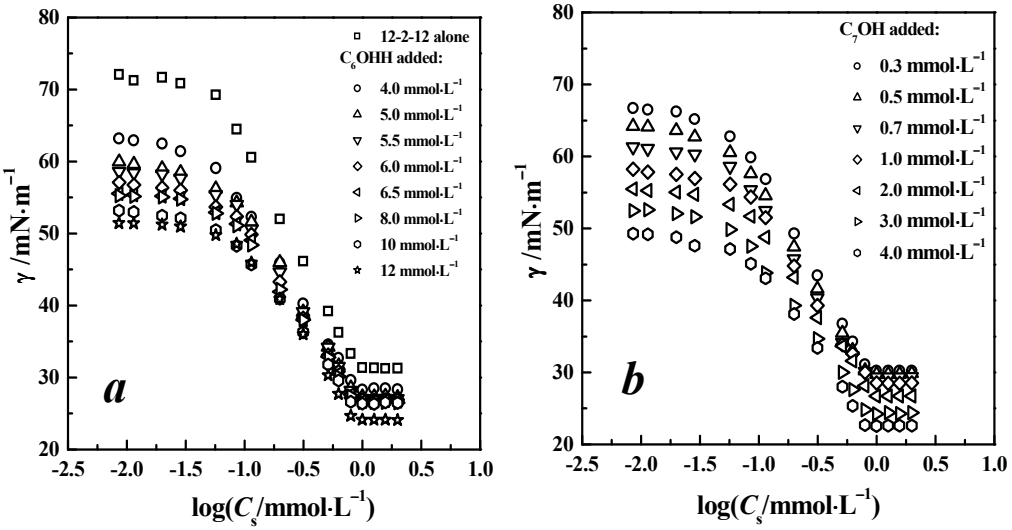

Fig.3 Semi-logarithmic plots of surface tension versus surfactant 12-2-12 concentration in the presence of C_6OH (***a***) and C_7OH (***b***) at 25°C

Table 1 Surface active parameters of surfactant systems at 25°C

systems	*cmc* ($mmol{\cdot}L^{-1}$)	C_{20} ($mmol{\cdot}L^{-1}$)	γ_{cmc} ($mN{\cdot}m^{-1}$)	$10^{10}\Gamma_{12\text{-}2\text{-}12}$ ($mol{\cdot}cm^{-2}$)	$10^{10}\Gamma_{COH}$ ($mol{\cdot}cm^{-2}$)	$10^{10}\Gamma_t$ ($mol{\cdot}cm^{-2}$)
12-2-12 alone	0.91	0.18	30.6	2.54	–	2.54 (5.08)
12-2-12 + C_6OH with a constant concentration ($mmol{\cdot}L^{-1}$):						
4.0	0.89	0.12	28.4	2.32	0.75	3.07 (5.39)
5.0	0.86	0.11	27.3	2.24	0.92	3.16 (5.40)
5.5	0.84	0.093	27.1	2.21	1.02	3.23 (5.44)

6.0	0.84	0.075	26.8	2.19	1.10	3.29 (5.48)
6.5	0.82	0.073	26.7	2.16	1.18	3.34 (5.50)
8.0	0.81	0.064	26.5	2.10	1.41	3.51 (5.61)
10.0	0.79	0.025	26.3	2.03	1.79	3.82 (5.85)
12.0	0.77	*	24.1	1.93	1.94	3.87 (5.80)
12-2-12 + C_7OH with a constant concentration ($mmol \cdot L^{-1}$):						
0.3	0.89	0.18	30.2	2.39	0.40	2.79 (5.18)
0.5	0.88	0.16	29.8	2.32	0.57	2.89 (5.21)
0.7	0.87	0.14	29.4	2.27	0.76	3.03 (5.30)
1.0	0.86	0.11	28.5	2.23	0.95	3.18 (5.41)
2.0	0.85	0.059	26.7	2.12	1.38	3.50 (5.62)
3.0	0.79	0.025	24.3	1.98	1.96	3.94 (5.92)
4.0	0.75	*	22.6	1.87	2.47	4.34 (6.21)

Note: * indicates where the alcohol itself made the surface tension of water reduced to over 20 $mN \cdot m^{-1}$. The data in parentheses are the total mole number of the alkyl tails ($\Gamma_{t,\ tails}$) at the interface per area unit (cm^2) including the alkyl tails of both 12-2-12 and alcohol.

3.3 Synergistic effect and mixed adsorption of 12-2-12/alcohol at the air/water interface

According to Rubingh-Rosen theory, the composition of a mixed adsorption monolayer (X_1^{σ} and X_2^{σ}, where the subscripts 1 and 2 stand for 12-2-12 and alcohol, respectively) and the molecular interaction parameter β^{σ} can be calculated by following formulas[27-29]

$$\frac{(X_1^{\sigma})^2 \ln(\alpha_1 C_{12} / X_1^{\sigma} C_1)}{(1-X_1^{\sigma})^2 \ln[(1-\alpha_1) C_{12} / (1-X_1^{\sigma}) C_2]} = 1 \quad (3)$$

$$\beta^{\sigma} = \frac{\ln(\alpha_1 C_{12} / X_1^{\sigma} C_1)}{(1-X_1^{\sigma})^2} \quad (4)$$

where C_1, C_2 and C_{12} are respectively the mole concentrations of 12-2-12, alcohol and their mixture in the bulk solution required to produce a given surface tension value, and α_1 and α_2 (=1−α_1) are the mole fractions of 12-2-12 and alcohol in the bulk solution on an active component only basis. The activity coefficients f_1^{σ} and f_2^{σ} of the surfactant and the alcohol in the mixed monolayer are related to β^{σ}

$$f_1^{\sigma} = \exp[\beta^{\sigma}(1 - X_1^{\sigma})^2] \quad (5)$$

$$f_2^{\sigma} = \exp[\beta^{\sigma}(X_1^{\sigma})^2] \quad (6)$$

β^{σ} indicates the deviation from ideality. For ideal mixing of two components, β^{σ} assumes a value of zero. A positive β^{σ} value means repulsive interactions amongst mixed species whereas a negative β^{σ} value corresponds to an attractive interaction. In addition, the value of β^{σ} also exhibits the degree of interaction between the two components within the adsorption monolayer, i.e. the more negative the value, the greater the interaction. In the current study, all β^{σ} values were negative (Table 2) suggesting that the interaction was more attractive between the two components in the monolayer than the self-interaction of each component before mixing. This phenomenon was consistent with the previous observation for the mixture of a similar gemini surfactant, butanediyl-1, 4-bis(cetyldimethylammonium bromide) (16-4-16), and identical alcohols[25].

The Gibbs equation can be used to calculate the surface excess Γ:

$$\Gamma = -\frac{1}{2.303nRT}\frac{d\gamma}{d\log C} \quad (7)$$

where n is a constant depending on the number of species adsorbed at the interface. In Fig.3, the semi-logarithmic plots of surface tension are represented as a function of the surfactant concentration and therefore Γ corresponds to the surface excess of 12-2-12 (Γ_s), where n is accounted for as 2, as suggested by other authors[30-33]. For 12-2-12 alone, Γ_s is 2.54×10^{-10} mol·cm^{-2}, which is close to that reported by Sikirić *et al*.[32] and Sun *et al*.[33]. Fig.4 shows a gradual decrease in Γ_s with competitively adsorbing alcohol molecules. This phenomenon agreed with the mixture of cetyltrimethylammonium bromide (CTAB) and propanol, where the adsorption of CTAB at the solution-air interface decreased with increasing propanol concentration[34].

The surface excess of alcohol Γ_a can be approximately estimated by following formula:

$$\frac{\Gamma_a}{\Gamma_s + \Gamma_a} = X_2^{\sigma} \quad (8)$$

As seen in Fig.4, Γ_a monotonously increased with addition of alcohol in the solution. Thus, total surface excess Γ_t (equal to the sum of Γ_s and Γ_a) kept rising with increasing concentration of alcohol in the bulk solution. Taking into account the two tails per gemini molecule, the total number of alkyl tails including both 12-2-12 and alcohol molecules absorbed at the air/water

interface per area-unit ($\Gamma_{t,\,tails}$) was calculated as the sum of $2\Gamma_s$ and Γ_a . The results are listed in the parentheses in the last line of Table 1. With the addition of alcohol in the solution, the $\Gamma_{t,\,tails}$ significantly increased and was always larger than that generated by 12-2-12 without additive. These results apparently indicate that the addition of alcohol promoted the formation of a more densely packed monolayer in comparison to that of 12-2-12 alone, agreeing with the role of linear alcohols in other surfactant systems[21-25]. Moreover, the C_7OH had higher efficiency than the C_6OH. For example, at a comparable concentration of 4.0 mmol·L^{-1} of alcohol, the $\Gamma_{t,\,tails}$ was 6.21 mol·cm^{-2} for C_7OH and 5.39 mol·cm^{-2} for C_7OH, respectively (Table 1). As emphasized in the introduction, the densely packed monolayer is an important basis for enhancing foam stability because it creates high interfacial elasticity and is subsequently discussed in more detail.

Table 2 Surface Composition (X^σ), activity coefficient (f^σ) and interaction parameter (β^σ) of binary mixtures of gemini surfactant 12-2-12 and alcohol calculated at 40 mN·m^{-1}

	α_2	X_1^σ	X_2^σ	f_1^σ	f_2^σ	β^σ
12-2-12 + C_6OH						
C_{C6OH}/mmol·L^{-1}						
4.0	0.918	0.757	0.243	0.948	0.598	–0.898
5.0	0.939	0.708	0.292	0.923	0.624	–0.940
5.5	0.947	0.684	0.316	0.907	0.633	–0.977
6.0	0.953	0.665	0.335	0.897	0.652	–0.967
6.5	0.958	0.647	0.353	0.887	0.670	–0.958
8.0	0.969	0.598	0.402	0.864	0.724	–0.903
10	0.979	0.532	0.468	0.822	0.777	–0.893
12	0.982	0.498	0.502	0.868	0.870	–0.563
12-2-12 + C_7OH						
C_{C7OH}/mmol·L^{-1}						
0.3	0.418	0.864	0.136	0.967	0.259	–1.811
0.5	0.573	0.802	0.198	0.928	0.297	–1.891
0.7	0.678	0.750	0.250	0.884	0.330	–1.972
1.0	0.772	0.701	0.299	0.844	0.393	–1.901

2.0	0.891	0.606	0.394	0.805	0.598	–1.399
3.0	0.944	0.502	0.498	0.712	0.708	–1.368
4.0	0.963	0.431	0.569	0.717	0.827	–1.025

Note: The C_{C6OH} and C_{C7OH} are the bulk concentrations of the corresponding alcohol in the solution. α_2 is the mole fraction of alcohol on an active-component-only basis. The subscripts 1 and 2 represent surfactant and alcohol, respectively.

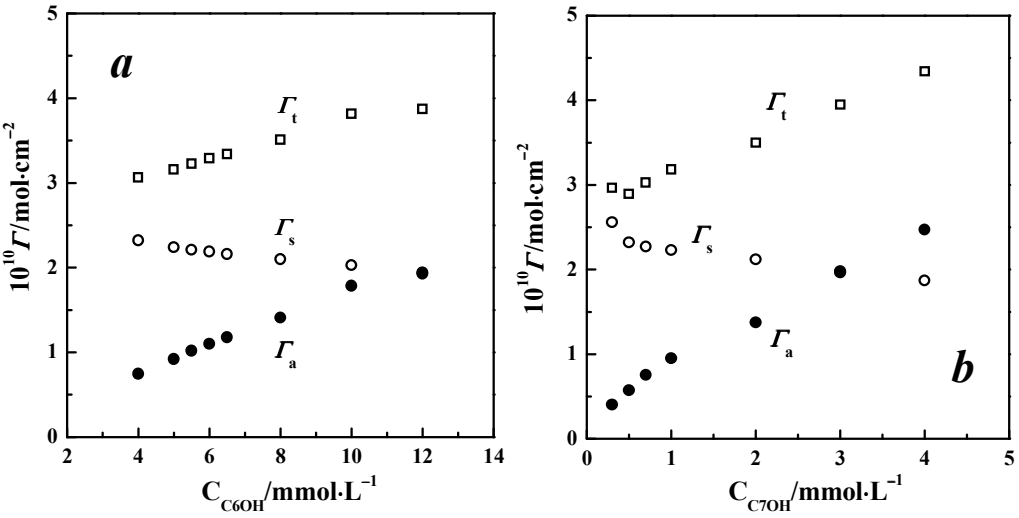

Fig.4 Surface excess as a function of the concentration of alcohol in bulk solution for (***a***) 12-2-12/C_6OH and (***b***) 12-2-12/C_7OH mixtures: (circles) Γ_s, (filled circles) Γ_a and (squares) Γ_t.

3.4 Dilational rheology of adsorption films

Previous studies have suggested that foam stability is closely related to the elasticity of the surfactant adsorbed film[5, 6, 8, 9, 11-13]. Briefly, the dilational behavior for a typical system of 12-2-12/0.7mmol·L^{-1}C_7OH at different surfactant concentrations is illustrated, others are available in the Supporting Information. Fig.5 shows the experimental plots of the complex dilational modulus ε^*, dilational elasticity ε, dilational viscosity η and phase angle θ as a function of the frequency of sinusoidal oscillation, All of these showed frequency dependence analogous to the previous observations[18-20]. The increasing disturbance frequency resulted in a decrease in the response time, over which the surfactant molecules exchanged between the interface and the bulk, and also moved inside the monolayer to restore equilibrium. At low frequencies, the time of the surfactant response was sufficient and thus various relaxation processes coming from diffusion

and adsorption of surfactants[35] and/or conformational changes of adsorbed molecules[36] can occur. At high frequencies, the response time was too short and the monolayer behaved as if it were insoluble. The phase angles were always positive for each of the mixtures over the range of examined frequencies, indicating that the phase of interfacial tension oscillation preceded that of the interfacial area oscillation.

In addition to frequency influence, the bulk concentration of surfactant also determined the viscoelastic behavior of the solutions, which are shown in Fig.6. At a designated frequency, the experimental ε and η run through a maximum with increasing surfactant concentration. This was similar to the behavior of both conventional surfactants[9, 14, 15, 37] and gemini surfactants[18-20] at the air/water interface. Generally, an increase in the surfactant concentration in the bulk solution could have two effects, one was to increase the interface excess Γ, which, in turn, led to a higher elasticity and the second was to accelerate the molecular exchange between bulk and interface. The fast exchange at high concentration tended to even out any interface tension gradient dγ, which decreased the interfacial elasticity. Thus at low concentrations, the increase in ε was dominant, whereas at high concentrations, ε decreased as the molecular exchange was speeded up. This "crossover" was mirrored in a maximum of $\varepsilon(C)$ curve.

3.5 LVT model description for the experimental data

The Lucassen-van den Tempel (LVT) model was most commonly used to describe the viscoelastic behavior of the soluble monolayer[38, 39]. This model assumed that the material transport involved in the adsorption kinetics was governed only by diffusion without energy barriers and was considered the instantaneous coupling between the interface rheology and adsorption kinetics. The model predicted the viscoelastic moduli through the following equations

$$\varepsilon(v,C) = \varepsilon_0 \frac{1+\xi}{1+2\xi+2\xi^2} \tag{9}$$

$$\eta(v,C) = \frac{\varepsilon_0}{2\pi v} \frac{\xi}{1+2\xi+2\xi^2} \tag{10}$$

with

$$\xi = \sqrt{\frac{\omega_0}{4\pi v}} \tag{11}$$

where ε_0 is the theoretical high-frequency limit of surface elasticity and ω_0 is the molecular exchange parameter. Fig.7 shows the fitting results for the system of 12-2-12/0.7mmol·L^{-1}C$_7$OH using eqs 9 and 10, in which the LVT model describes the experimental data accurately.

According to the LVT model, at low frequencies, the dilational interfacial elasticity was close to zero, irrespective of the concentration of surfactant in the bulk phase as seen in Fig.S16. This could be explained as the interfacial tension gradient resulting from interface deformation almost vanished during the experimental time. At high frequencies, the dilational elasticity showed little change with further increasing frequency. Over this range, the work frequency was significantly higher than the characteristic frequency of the various relaxation processes occurring at and near the interface, and thus the interface film embodied the character of insoluble film. By eq.(11), ξ approaches to 0 when $\nu \to \infty$, and thus $\varepsilon = \varepsilon_0$ according to eq. 9. This procedure appeared simplistic but the high-frequency limit of elasticity could not often be determined since the high-frequency limit was not included experimentally. Thus the fitting parameters $\varepsilon_{0,\mathrm{fit}}$ and $\omega_{0,\mathrm{fit}}$ were considered to substitute for ε_0 and ω_0. The fitting procedure was carried out so that the couples of $\varepsilon_{0,\mathrm{fit}}$ and $\omega_{0,\mathrm{fit}}$ values best described both the experimental $\varepsilon(\nu, C)$ and $\eta(\nu, C)$ curves. Table S3 lists the fitting results for several of the typical systems. As revealed in Fig.7, the $\varepsilon_{0,\mathrm{fit}}$ was also concentration-dependent analogous to ε_0.

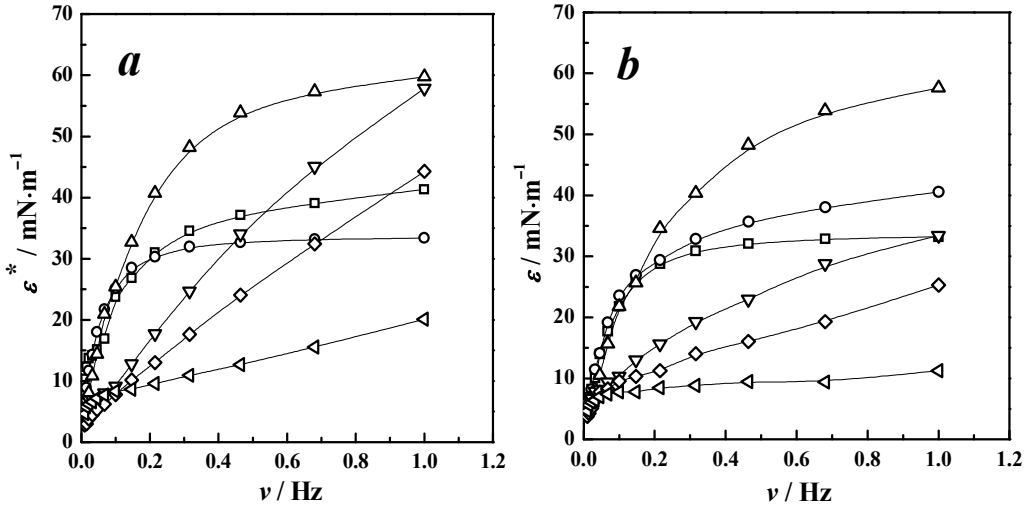

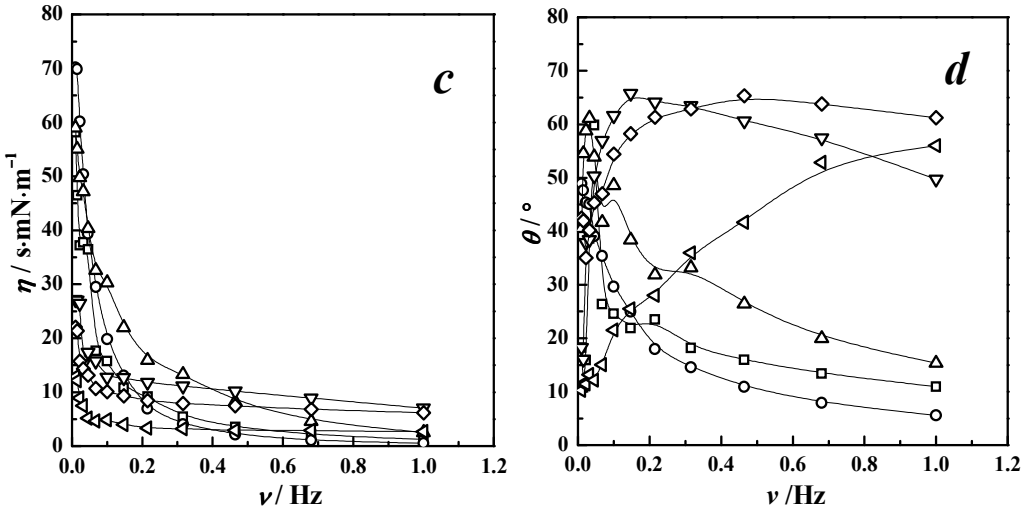

Fig.5 Experimental plots of complex modulus (ε^*, ***a***), interfacial elasticity (ε, ***b***), interfacial viscosity (η, ***c***) and phase angle (θ, ***d***) as a function of frequency (ν), respectively, for the mixed adsorption films in 12-2-12/0.7 mmol·L^{-1}C_7OH aqueous solutions at 25°C. The symbols represent different surfactant concentrations: log(C/mmol·L^{-1}) = –1.38 (□), –1.18 (○), –0.93 (△), –0.63 (▽), –0.52 (◇), –0.30 (◁)

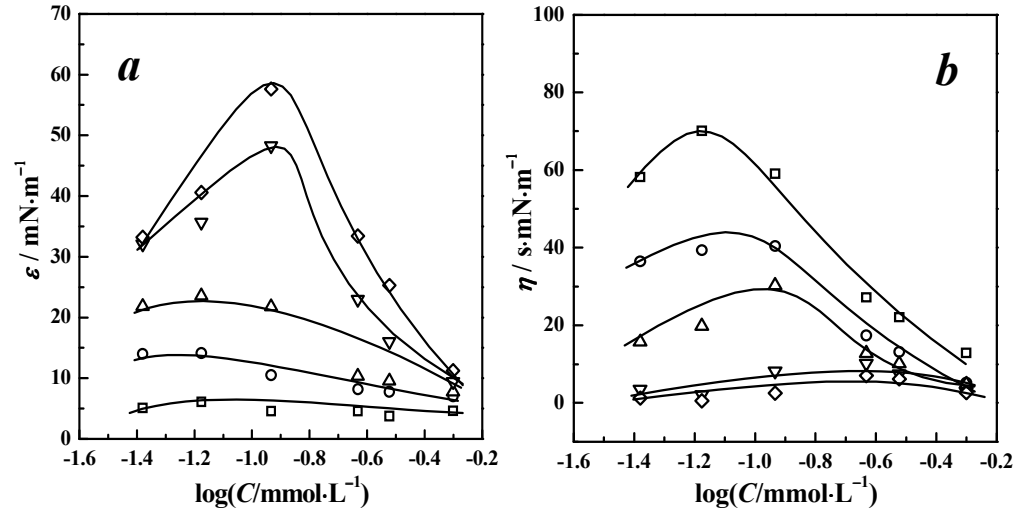

Fig.6 Semi-logarithmic plots of dilational interfacial elasticity (ε, ***a***) and interfacial viscosity (η, ***b***) as a function of the surfactant concentration C for 12-2-12/0.7 mmol·L^{-1}C_7OH aqueous solutions. The symbols indicate different frequencies: ν/Hz = 0.010 (□), 0.046 (○), 0.100(△),0.464 (▽) and 1.000 (◇)

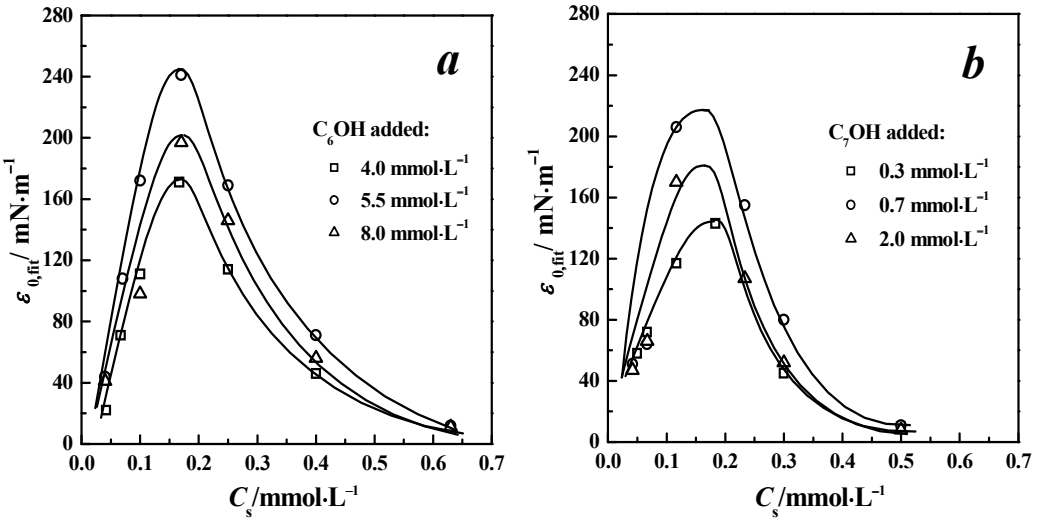

Fig.7 Concentration dependent plots of high-frequency limit elasticity $\varepsilon_{0,fit}$ for (***a***) 12-2-12/C_6OH and (***b***) 12-2-12/C_7OH mixtures

3.6 Film elasticity and foam stability

In the studies a relationship between the foam stability and the elasticity of the film has been shown[18-20]. High interfacial elasticity is closely related to high foam stability. However, it was noticed that in this relationship the interfacial elasticity should choose its high-frequency limit where the influence of frequency can be excluded. For 12-2-12/C_6OH mixtures, Fig.7a shows that at a comparable surfactant concentration, the $\varepsilon_{0,fit}$ in the presence of 5.5mmol·L^{-1} alcohol was always larger than the other two $\varepsilon_{0,fit}$ generated in the presence of 4.0 and 8.0 mmol·L^{-1} C_6OH. Similarly, for 12-2-12/C_7OH mixtures, the $\varepsilon_{0,fit}$ in the presence of 0.7mmol·L^{-1} alcohol was also the largest at comparable surfactant concentrations (Fig.7b). This explained that the optimum effect of adding alcohols in enhancing foam stability was at 5.5mmol·L^{-1} for C_6OH and 0.7 mmol·L^{-1} for C_7OH, respectively, as shown in Fig.2.

As indicated in previous studies[18-20], a more quantitative analysis should be based on the limit of elasticity obtained on the level of identical surface excesses rather than that of the same concentrations in the bulk solution[14, 18-20]. For this purpose, we plotted the adsorption isotherms with a Frumkin-form (Fig.8), which were derived from fitting the surface tension data by Szyszkowski formula and then calculating the surface excesses by the Gibbs equation[27]. Combining Figs.7 and 8, at an identical surface excess of 2×10^{-10} mol·cm^{-2}, the $\varepsilon_{0,fit}$ was 218 mN·m^{-1} for 12-2-12/0.7mmol·$L^{-1}$$C_7$OH and 195 mN·$m^{-1}$ for 12-2-12/5.5mmol·$L^{-1}$$C_6$OH,

respectively. The larger $\varepsilon_{0,fit}$ for the C_7OH system than that for the C_6OH system mirrored the higher foam stability for the former as indicated in section 3.1.

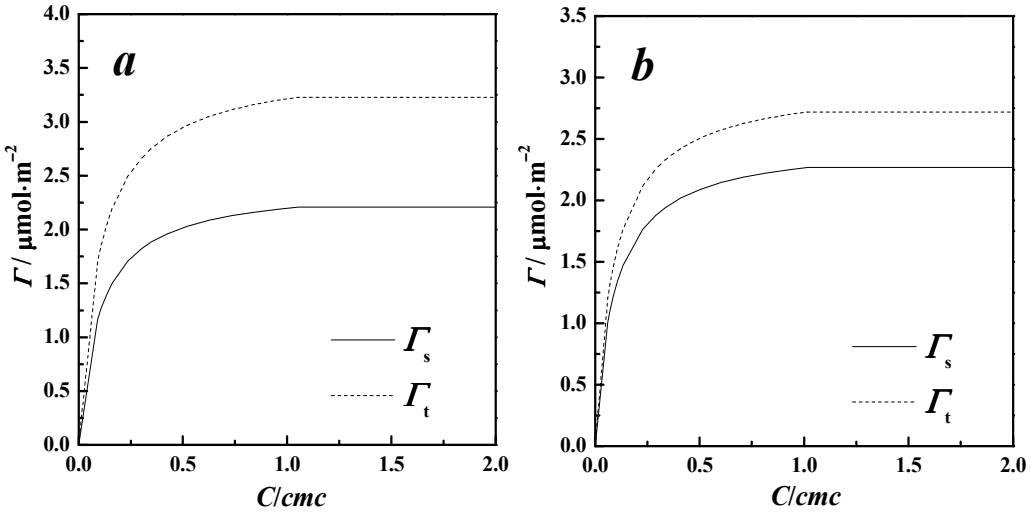

Fig.8 Frumkin adsorption isotherms for 12-2-12/5.5mmol·$L^{-1}$$C_6OH$ (***a***) and 12-2-12/0.7mmol·$L^{-1}$$C_7OH$ (***b***) mixtures

4. Conclusions

This paper investigated highly stable foam systems generated by a cationic gemini surfactant, ethanediyl-1, 2-bis(dodecyldimethylammonium bromide) (12-2-12), together with a linear alcohol, hexanol (C_6OH) or heptanol (C_7OH). The maximum half-life $t_{1/2,max}$ of bubbles attained 1413 min for 12-2-12/5.5mmol·$L^{-1}$$C_6OH$ and 1497 min for 12-2-12/0.7mmol·$L^{-1}$$C_7OH$, which were two-fold higher than that stabilized by 12-2-12 without additives. The added alcohol can further fill in the gaps of the monolayers formed by the gemini surfactant with a short spacer, producing more stable foams. The adsorption and interfacial rheology measurements reveal that the foam stability is closely related to the surface activity and interfacial elasticity of the mixed systems. Addition of alcohols decreases the *cmc* and γ_{cmc} of 12-2-12, indicating the aggregation and adsorption of mixed systems are greatly enhanced because of the synergistic effect of alcohols with 12-2-12. All values of interaction parameter β^{σ} for mixed systems are negative, suggesting the presence of attractive interactions between the two components in the monolayer. At an identical surface excess of 2×10^{-10} mol·cm^{-2}, the $\varepsilon_{0,fit}$ obtained by fitting interfacial rheology data with LVT model was 218 mN·m^{-1} for 12-2-12/0.7mmol·$L^{-1}$$C_7OH$ and 195 mN·m^{-1} for 12-2-12/5.5mmol·$L^{-1}$$C_6OH$, respectively. These results reveal that 12-2-12/C_7OH systems can generate more stable foams at

lower alcohol concentrations than that of 12-2-12/C_6OH, indicating that alcohols with longer alkyl tail length are more effective additives in stabilizing foams. The obtained results suggest a new formula to generate highly stable foams using a gemini surfactant with a short spacer together with a linear alcohol. The systems presented have potential wide ranging applications in the construction of new complex fluids.

Acknowledgments

Support from the National Natural Science Foundation of China (Grants No. 21473032 and 21273040) is gratefully acknowledged.

References

1 T. R. Kuang, H. Y. Mi, D. J. Fu, X. Jing, B. Y. Chen, W. J. Mou and X. F. Peng, *Ind Eng Chem Res*, 2015, 54, 758-768.

2 J. L. Toca-Herrera, N. Krasteva, H. J. Muller and R. Krastev, *Adv Colloid Interface Sci*, 2014, 207, 93-106.

3 J. L. Joye, G. Hirasaki, C. A.,Miller. *Langmuir,* 1994, 10, 3174-3179.

4 J. L. Joye, G. Hirasaki, C. A. Miller, *J. Colloid Interface Sci.,* 1996, 177, 542-552.

5 A. Sonin, A. Bonfillon, LD. angevin, *J. Colloid Interface Sci.,* 1994, 162, 323-330.

6 A. Espert, R. V. Klitzing, P. Poulin, A. Colin, R. Zana, D. Langevin, *Langmuir,* 1998, 14, 4251-4260.

7 H. Fruhner, K. D. Wantke, K. Lunkenheimer, *Colloids Surf. A,* 1999, 162, 193-202.

8 V. Bergeron, *Langmuir,* 1997, 13, 3474-3482.

9 C. Stubenrauch, R. Miller, *J. Phys. Chem. B,* 2004, 108, 6412-6421.

10 P. Koelsch, H. Motschmann, *Langmuir,* 2005, 21, 6265-6269.

11 E. Santini, F. Ravera, M. Ferrari, C. Stubenrauch, A. Makievski, J. Krägel, *Colloids Surf. A,* 2007, 298, 12-21.

12 L. Wang, R. H. Yoon, *Int. J. Miner. Process,* 2008, 85, 101-110.

13 D. Georgieva, A. Cagna, D. Langevin, *Soft Matter,* 2009, 5, 2063-2071.

14 F. Monroy, J. Giemanska-Kahn, D. Langevin, *Colloids Surf. A,* 1998, 143, 251-260.

15 C. Stenvot, D. Langevin, *Langmuir,* 1988, 4, 1179-1183.

16 F. M. Menger, C. A. Littau, *J. Am. Chem. Soc.,* 1991, 113, 1451–1452.

17 E. Alami, G. Beinert, P. Marie, R. Zana, *Langmuir*, 1993, 9, 1465-1467.

18 X. N. Wu, J. X. Zhao, E. J. Li, W. S. Zou, *Colloid Polym. Sci.,* 2011, 289 (9), 1025-1034.

19 Y. You, X. N. Wu, J. X. Zhao, Y. Z. Ye, W. S. Zou, *Colloids Surf. A*, 2011, 384, 164-171.

20 X. N. Wu, W. S. Zou, J. X. Zhao, *Acta Phys-Chim Sin,* 2012, 28, 1213-1217.

21 B. D. Casson, C. D. Bain, *J. Phys. Chem. B,* 1999, 103, 4678-4686.

22 M. Villeneuve, N. Ikeda, K. Motomura, M. Aratono, *J. Colloid Interface Sci.,* 1998, 204, 350-356.

23 H. Matsubara, T. Eguchi, H. Takumi, K. Tsuchiya, T. Takiue, M. Aratono, *J. Phys. Chem. B,* 2009, 113, 8847-8853.

24 R. Mohammad, I. A. Khan, Kabir-ud-Din, P. C. Schulz, *J. Molecular Liquids,* 2011, 162, 113-121.

25 I. A. Khan, R. Mohammad, S.Alam, Kabir-ud-Din, *J. Disp. Sci. Tech.,* 2010, 31, 129-137.

26 A. R. Tehrani-Bagha, K. Holmberg, *Langmuir,* 2010, 26, 9276-9282.

27 M. J. Rosen, *Surfactants and Interfacial Phenomena*, 2nd ed., John Wiley & Sons Inc., 1988

28 Rubingh, D. N. in *Solution Chemistry of Surfactants*, Mittal, K. L. (Ed.), Vol. 1, Plenum, New York, 1979, pp.337-354.

29 M. J. Rosen, X. Y. Hua, *J. Colloid Interface Sci*., 1982, *86*, 164.

30 R. Zana, *J. Colloid Interface Sci.,* 2002, 248, 203-220.

31 Z. X. Li, C. C. Dong, R. K. Thomas, *Langmuir,* 1999, 15, 4392-4396.

32 M. Sikirić, I. Primožič, N. Filipović-Vinceković, *J. Colloid Interface Sci.,* 2002, 250, 221-229.

33 Y. Sun, Y. Feng, H. Dong, Z. Chen, L. Han, *Central Euro. J. Chem.,* 2007, 5, 620-634.

34 A. Zdziennicka, B. Hańczuk, *J. Colloid Interface Sci.,* 2008, 317, 44-53.

35 J. Lucassen, M. van den Tempel, *Chem. Eng. Sci.,* 1972, 27, 1283-1291.

36 F. Monroy, S. Rivillon, F. Ortega, R. G. Rubio, *J. Chem. Phys.,* 2001, 115, 530-539.

37 V. I. Kovalchuk, J. Krägel, A. V. Makievski, F. Ravera, L. Liggieri, G. Loglio, V.B. Fainerman, R. Miller, *J. Colloid Interface Sci.,* 2004, 280, 498-505.

38 J. Lucassen, M. van den Tempel, *Chem. Eng. Sci.,* 1972, 27, 1283-1291.

39 J. Lucassen, M. van den Tempel, *J. Colloid Interface Sci.,* 1972, 41, 491-498.